

---

# Make Autoregressive Great Again: Diffusion-Free Graph Generation with Next-Scale Prediction

---

Samuel Belkadi\*

University of Cambridge  
sb2764@cam.ac.uk

Steve Hong\*

University of Cambridge  
mdh58@cam.ac.uk

Marian Chen\*

University of Cambridge  
mc2509@cam.ac.uk

## Abstract

Autoregressive models are popular generative models due to their speed and properties. However, they require an explicit sequence order, which contradicts the unordered nature of graphs. In contrast, diffusion models maintain permutation invariance and enable one-shot generation but require up to thousands of denoising steps and additional features, leading to high computational costs. Inspired by recent breakthroughs in image generation—especially the success of visual autoregressive methods [1, 2]—we propose MAG, a novel diffusion-free graph generation framework based on next-scale prediction. By leveraging a hierarchy of latent representations, the model progressively generates scales of the entire graph without the need for explicit node ordering. Extensive experiments on both generic and molecular graph datasets demonstrate that MAG delivers competitive performance compared to state-of-the-art methods, achieving up to three orders of magnitude in speedup during inference.

## 1 Introduction

Graphs provide a natural and flexible information representation across a wide range of domains, including social networks, biological and molecular structures, recommender systems, and infrastructural networks. Consequently, the ability to learn a graph distribution from data and generate realistic graphs is pivotal for applications such as network science, drug discovery, and protein design.

Despite significant progress in generative models for language and images, graph generation remains challenging due to its inherent combinatorial nature. Specifically, graphs are naturally **high-dimensional** and **discrete** with **varying sizes**, contrasting with the continuous space and fixed-size techniques that cannot be directly applied to them. Furthermore, rich substructures in graphs necessitate an expressive model capable of capturing **higher-order** motifs and interactions.

Several graph generative models have been proposed to address some of these challenges, undertaking approaches based on autoregressive (AR) models [3], variational autoencoders (VAE) [4], generative adversarial networks (GAN) [5], and diffusion models [6–8]. Among these, diffusion and autoregressive models stand out with superior performance and interesting properties [9–11].

On one hand, diffusion models offer the ability to achieve exchangeable probability in combination with permutation equivariant networks, under certain conditions [6, 7]. However, given the high-dimensional nature of graphs and their complex internal dependencies, directly modeling the joint distribution of all nodes and edges presents significant challenges. Recent work by Zhao et al. [10] demonstrates that, as a cost for permutation invariance, capturing the full joint distribution and solving the transformation difficulty via diffusion requires thousands of sampling and denoising steps as well as additional node-, edge-, and graph-level features, such as eigenvectors, to break symmetries and achieve high generation quality, rendering diffusion a promising but very expensive approach.

On the other hand, in addition to their improved **efficiency**, studies into the success of AR models have highlighted their **scalability** and **generalizability**. The former, as exemplified by scaling laws [12],

---

\*Equal contribution.

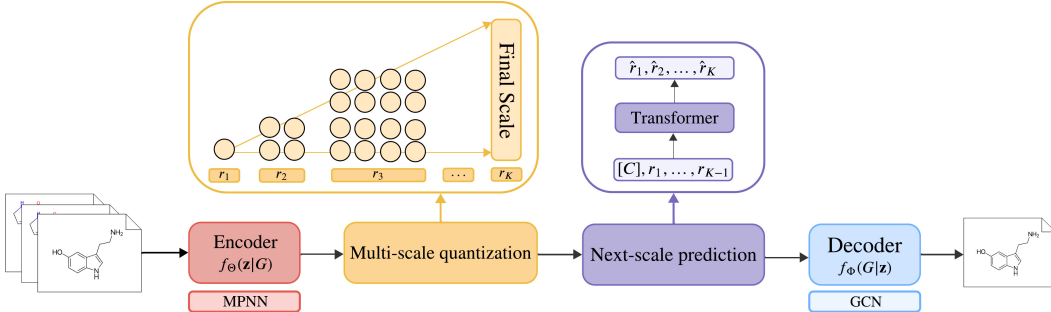


**Figure 1: Overview of the Multi-Scale Graph Generation Framework.** The input graph is first encoded through an MPNN, which produces a latent representation that is quantized at multiple scales. A Transformer then predicts the scales autoregressively via a coarse-to-fine next-scale process, and a GCN-based decoder reconstructs the graph from the final discrete latent representation  $r_K$ .

allows the prediction of large models’ performance to better guide resource allocation during training, while the latter, as evidenced by zero-shot and few-shot learning [13], underscores the adaptability of unsupervised-trained models to unseen tasks. Furthermore, the aforementioned **discrete** and **varying-size** properties of graphs suggest a promising fit for autoregressive modeling. However, unlike natural language sentences with an inherent left-to-right ordering, the order of nodes in a graph must be explicitly defined for unidirectional autoregressive learning. Previous AR methods [3, 14, 15] attempted to enforce node ordering or approximate the marginalization over permutations such that, once flattened, one can train an autoregressive model to maximize its likelihood via next-token prediction. This gives rise to the three main issues of autoregressive graph generation:

1. **Long-range bottleneck.** Generating nodes one at a time results in sequential dependencies that make it difficult to capture long-range interactions and global structures. Furthermore, early predictions errors can propagate throughout the generation process, and dependencies may decay when working on larger graphs.
2. **Counterintuitive node ordering.** Enforcing a specific node ordering is at odds with the inherent invariance of graphs, forcing the model to learn over a specific ordering, thereby increasing complexity and reducing generalization.
3. **Inefficiency.** Generating a graph sequence  $(x_1, x_2, \dots, x_{N \times N})$  with a conventional self-attention transformer incurs  $\mathcal{O}(n^2)$  autoregressive steps and  $\mathcal{O}(n^3)$  computational cost.

Drawing inspiration from recent breakthroughs in image generation—notably the Visual Autoregressive Modeling (VAR) framework [1, 2]—our proposed method introduces a new ordering for graphs that is **multi-scale, coarse-to-fine**. We define autoregressive learning for graphs as *next-scale* prediction instead of traditional *next-node* and *next-edge* approaches, thereby infusing autoregressive properties with graphs’ structural constraints. As exemplified in Figure 1, our method first encodes a graph into multiple scales of latent representations and learns to generate scales autoregressively, starting from a singular token map and progressively expanding its resolution. At each step, a transformer predicts the next-resolution token map, conditioned on all previous scales and a class label  $[C]$  for conditional synthesis.

MAG poses significant improvements over traditional AR methods on both generic and molecular graph datasets within all experiments. Notably, it closes the gap with diffusion baselines, surpassing them in data efficiency, training time, inference speed, and scalability, with only little overhead in performance. This provides strong evidence regarding the effectiveness of next-scale prediction for scalable and high-quality graph generation. In summary, our contributions are threefold:

1. A novel next-scale prediction framework for hierarchical graph generation that overcomes the limitations of traditional autoregressive approaches on graphs properties.
2. A thorough theoretical and empirical analysis of how multi-scale latent representations can effectively capture high-order motifs while remaining significantly more efficient than counterparts.
3. Experiments on diverse graph datasets, demonstrating significant improvements over AR baselines and little performance overhead compared to state-of-the-art diffusion methods.

## 2 Related Work

**Diffusion and score-based models.** Diffusion models achieve permutation-invariance by parameterizing the denoising/score function with a permutation equivariant network, at the cost of up to thousands of sampling steps. EDP-GNN [6] is the first work to adapt score-based models to graph generation by representing graphs as matrices with continuous values. GDSS [7] generalizes this approach by leveraging SDE-based diffusion and replacing adjacency matrices with node and edge features. However, by using continuous-state diffusion, these approaches ignore graphs’ discrete nature, resulting in fully connected graphs. DiGress [8] is the first to apply discrete-state diffusion, achieving significant improvements over continuous methods; yet, they require additional structural and domain-specific features to break symmetries and achieve high generation quality, further increasing computational costs. In response, SwinGNN [11] argues that learning exchangeable probabilities with equivariant architectures is challenging, instead proposing fixed node orderings and non-equivariant score functions to alleviate complexity while maintaining competitive performance.

**Autoregressive models.** Traditional AR models construct graphs by adding nodes and edges sequentially. Although this approach aligns with the discrete nature of graphs, it faces a fundamental challenge, as there is no inherent order in graph generation. Various strategies have been explored to address this by enforcing some node ordering and approximating the marginalization over permutations. Li et al. [16] suggest using random or deterministic empirical orderings. GraphRNN [3] aligns permutations with Breadth-First Search (BFS) ordering through a many-to-one mapping. GRANs [14] propose an approach to marginalize over a family of canonical node orderings, such as node degree descending, BFS trees rooted at the highest degree node, and k-core orderings. Chen et al. [17] eliminate ad-hoc orderings altogether by modeling the conditional probability of orderings with another AR model to estimate the marginalized probabilities for both the generative and ordering-selection models. Despite these efforts, all such methods remain fundamentally limited by the need to impose artificial node orderings.

**Hybrid and hierarchical models.** Hybrid models attempt to combine diffusion and AR models to balance performance and speed. PARD [10] decomposes graph generation into blocks before applying diffusion within each block and AR between them, while ensuring permutation invariance through *partial ordering*. However, block-wise diffusion may introduce implementation complexity and remain limited by sampling efficiency [18]. In contrast, GraphArm [9] employs an AR diffusion model where, at each forward step, exactly one node and its adjacent edges decay to absorbing states based on a random node ordering, making the model both permutation- and order-sensitive. Coarse-to-fine graph generation has also been explored. Bergmeister et al. [19] generate a full graph from a single node through localized denoising diffusion and spectral conditioning, achieving high performance but with generation times similar to those of full diffusion models. Meanwhile, JT-VAE [4] and HierVAE [20] generate graphs hierarchically using chemically valid molecular substructures, making these methods only viable on molecular tasks. Lastly, HiGGs [21] introduce a hierarchical framework that leverages GNNs with conditional generation capabilities to sample graphs across multiple resolution levels and extend the scale of the generated graphs with respect to training inputs.

## 3 Method

Consider a graph defined by the quadruple  $G = (\mathcal{V}, E, \mathbf{X}, \mathbf{E})$ , where  $\mathcal{V}$  denotes the set of  $N$  vertices,  $E \subseteq \mathcal{V} \times \mathcal{V}$  represents the set of edges,  $\mathbf{X} \in \mathbb{R}^{N \times D}$  is the matrix containing  $D$ -dimensional node features, and  $\mathbf{E} \in \mathbb{R}^{N \times N \times F}$  comprises edge attributes with feature dimensions  $F$ . Given a collection of  $M$  observed graphs,  $\mathcal{G} = \{G_i\}_{i=1}^M$ , the task of graph generation is to model the underlying distribution  $p(\mathcal{G})$  in order to generate new graphs  $G_{\text{sample}} \sim p(\mathcal{G})$ .

### 3.1 Preliminary: Autoregression by Scale

AR models represent the joint distribution over  $N$  random variables by employing the chain rule of probability. In particular, they decompose the generation process into sequential steps, where each step determines the subsequent action based on the current subgraph. Traditionally, previous works have taken a *next-token prediction* approach, generating the graph one node and its incident edges at a time. Specifically, at step  $i$ , we introduce node  $G_i^\pi$  along with any new edges connecting it to nodes

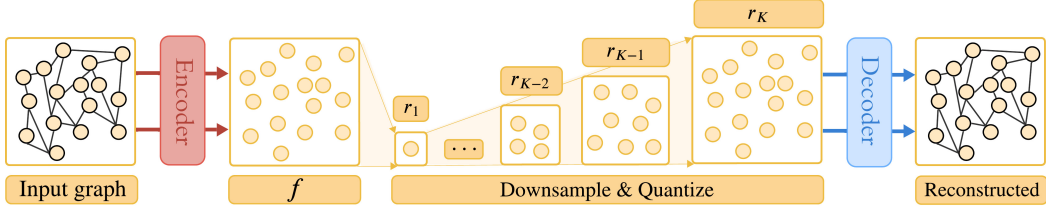


**Figure 2: Permutation Equivariant Multi-Scale VQ-VAE.** The encoder converts the input graph into a continuous latent representation  $f$ , which is downsampled and quantized into discrete token maps  $\{r_1, \dots, r_K\}$ . The final token map  $r_K$  is then passed to the GCN-based decoder to reconstruct the original graph, preserving permutation equivariance throughout.

in  $\{G_1^\pi, G_2^\pi, \dots, G_{i-1}^\pi\}$ . The general formulation of AR models for graphs is given by:

$$p(\mathcal{G}^\pi) = \prod_{i=1}^N p(G_i^\pi | G_1^\pi, G_2^\pi, \dots, G_{i-1}^\pi).$$

Since AR models proceed in a unidirectional sequential manner, applying them requires a predetermined ordering  $\pi$  of nodes in the graph.

Alternatively, rather than employing *next-token prediction*, we suggest utilizing *next-scale prediction*, wherein the autoregressive unit is a latent representation of the entire graph rather than a single token. To implement this, we first obtain latent representations at multiple scales and train a transformer to generate these latent maps. Similarly to Tian et al. [1], this leads to a two-stage architecture: (1) a VQ-VAE tokenizer that quantizes the input graphs into latent maps at multiple scales (detailed in Section 3.2), and (2) a transformer that predicts next-scale latent maps (discussed in Section 3.3).

### 3.2 Permutation Equivariant Multi-Scale Tokenizer

We propose a permutation-equivariant quantized autoencoder to encode a graph  $G$  to  $K$  multi-scale discrete latent maps  $R = \{r_1, r_2, \dots, r_K\}$ , where each scale  $r_k$  depends only on its prefix  $\{r_1, r_2, \dots, r_{k-1}\}$ . For quantization, a shared codebook  $Z$  is used across all scales, ensuring that each token in  $r_k$  belongs to the same vocabulary. An overview of the tokenizer is given in Figure 2.

**Encoding.** Given an input graph  $G \in \mathbb{R}^{N \times D} \times \mathbb{R}^{N \times N \times F}$ , an autoencoder  $\mathcal{E}(\cdot) : \mathbb{R}^{N \times D} \times \mathbb{R}^{N \times N \times F} \rightarrow \mathbb{R}^{N \times C}$  is used to convert  $G$  into a continuous latent representation  $f$ :

$$f = \mathcal{E}(G), \quad f \in \mathbb{R}^{N \times C},$$

where  $C$  is the latent's feature dimension defined empirically. In order to encode the graph's node and edge features into a unified latent space  $\mathbb{R}^{N \times C}$ , we leverage a series of MPNNs, such that edge features are propagated within node features before compressing node dimensions to  $C$  and dropping remaining edges.

$f$  is then downsampled to create  $K$  different coarse-to-fine latent scales  $F = \{f_1, f_2, \dots, f_K\}$ , with  $f_K = f$ . Intermediate scales are learned by the model to autoregressively generate the graph's latent representation, scale-wise.

**Quantizing.** A quantizer is used to convert each scale's latent representation into discrete tokens. The quantizer  $\mathcal{Q}(\cdot) : \mathbb{R}^{N \times C} \rightarrow \mathbb{R}^{N \times C_Z}$  includes a codebook  $Z \in \mathbb{R}^{V \times C_Z}$  containing  $V$  learnable embeddings, for which each feature's dimension is maintained by convention, i.e.,  $C_Z = C$ . During quantization,  $q = \mathcal{Q}(f)$  is obtained by replacing each feature vector  $f^{(k,i)}$  from the multi-scale latent features  $F$  by its nearest code  $q^{(k,i)}$  in Euclidean distance:

$$q^{(k,i)} = (\operatorname{argmin}_{v \in V} \|\operatorname{Select}(Z, v) - f^{(k,i)}\|_2) \in V,$$

where  $\operatorname{Select}(Z, v)$  denotes selecting the  $v^{th}$  vector in codebook  $Z$ ,  $k \leq K$  and  $i \leq N$ .  $\mathcal{Q}(\cdot)$  is trained by fetching all  $q^{(k,i)}$ , given  $F$ , and minimizing the distance between  $q$  and  $f$ .

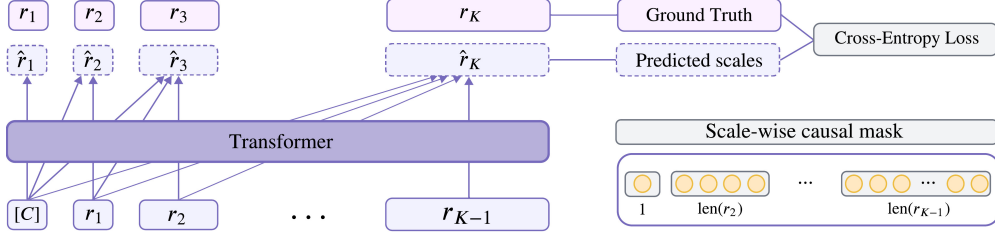


**Figure 3: Autoregressive Next-scale Prediction with Scale-wise Causal Mask.** At each step  $k$ , the transformer attends to all previously generated scales  $\{r_1, \dots, r_{k-1}\}$  and predicts the next-scale token map  $r_k$  all at once. A scale-wise causal mask ensures that each scale only depends on its prefix. Cross-entropy loss is used for training the transformer.

**Decoding.** Finally, a decoder is used to reconstruct the original graph given its final discrete latent representation,  $r_K$ . The decoder  $\mathcal{D}(\cdot) : \mathbb{R}^{N \times C_Z} \rightarrow \mathbb{R}^{N \times D} \times \mathbb{R}^{N \times N \times F}$  recovers latent representations for edges between all pairs of nodes, and maps node and edge features back to their original dimensions  $\mathbb{R}^{N \times D}$  and  $\mathbb{R}^{N \times N \times F}$ , respectively.

Because this architecture preserves node ordering and feature cardinality throughout encoding, quantization, and decoding, the proposed multi-scale autoencoder remains **permutation equivariant**. Note that any off-the-shelf autoencoder can be used, since downsampled scales are obtained by interpolating, and only the embedding  $f$  (and thus final scale  $r_K$ ) is used for decoding. This effectively makes the scales independent of the rest of the architecture.

### 3.3 Autoregressive Graph Generation Through Next-Scale Prediction

We define the autoregressive modeling on graphs by shifting from *next-node* and *next-edge* predictions to *next-scale* predictions. Here, the autoregressive unit is *an entire token map*, rather than *a single token*. Given the quantized scales  $\{r_1, r_2, \dots, r_K\}$ , the autoregressive likelihood is formulated as:

$$p(r_1, r_2, \dots, r_K) = \prod_{k=1}^K p(r_k | r_1, r_2, \dots, r_{k-1}),$$

where each autoregressive unit  $r_k \in [V]^{n_k}$  is the token map at scale  $k$  containing  $n_k$  tokens, and the sequence  $(r_1, r_2, \dots, r_{k-1})$  serves as the prefix for  $r_k$ . In the  $k$ -th autoregressive step, we predict the  $k$ -th scale, such that all  $n_k$  tokens in  $r_k$  are generated in parallel, conditioned on  $r_k$ 's prefix. Note that during training, a block-wise causal attention mask is used to ensure that each  $r_k$  can only attend to its prefix  $r_{<k}$ . During inference, kv-caching is used and no mask is needed. An overview of the generative model's architecture is displayed in Figure 3.

**Level embedding.** A level embedding is learned to encode the scale at which a token operates within the input structure. This is implemented similarly to GPT's segment embedding [22], such that learned signals enhance the model's capacity to capture multi-scale contextual dependencies.

**Scale sampling.** During training, we uniformly sample  $K$  scale sizes to enhance the model's generalization ability to perceive any scale. Specifically, we set the maximum number of scales to  $K_{\max}$  based on the task, and fix the first scale to 1 and the last to  $N$ , where  $N$  is the desired graph size. Intermediate scale sizes are uniformly sampled. During inference, we set all scales to predefined sizes (e.g.,  $R = \{1, 2, 4, 6, 9\}$ ) and generate them autoregressively, such that  $\forall r_k \in R, r_k \leq N$  and the final scale  $r_K = N$  (e.g., truncating to  $\{1, 2, 4, 5\}$  for a graph of 5 nodes).

**Implementation details.** We adopt a standard decoder-only transformer architecture with adaptive layer normalization (AdaLN). For class-conditional synthesis, the class embedding is used as the start token  $[C]$  and the condition of AdaLN. We do not use any advanced positional embeddings, such as those delineated in Graphomer [23] or DiGress [8].

**Discussion.** Multi-scale prediction offers substantial properties that allow MAG to address the three previously mentioned issues as follows:

- Given the limited number of intermediate scales in the generations, long-range dependency is reduced from  $\mathcal{O}(n^2)$  to  $\mathcal{O}(k)$ , where  $k \approx \log(n)$  is the number of scales. Furthermore, sequential dependency is strengthened by generating a scale of the whole graph at each autoregressive step.
- No explicit node ordering is required, as (i) the tokenizer is permutation equivariant, and (ii) tokens in each map  $r_k$  are fully correlated and generated in parallel.
- By generating an entire token map in parallel at each scale, the generation's complexity is reduced from  $\mathcal{O}(n^3)$  to  $\mathcal{O}(kn^2)$ , where  $k \approx \log(n)$ . The proof is detailed in Appendix A.

## 4 Experiments

We empirically evaluate our model on experiments covering both generic and molecular graph generation. These two domains are chosen to benchmark the model's versatility: generic graphs allow the assessment of structural fidelity and scalability, while molecular graphs pose domain-specific challenges like chemical validity and functional constraints. This dual setting probes MAG's ability to generate diverse, high-quality graphs under different structural and semantic constraints.

Generation quality is measured using a combination of distributional and domain-specific metrics. Moreover, we evaluate generation time against state-of-the-art diffusion, hybrid, and VAE models to compare their inference efficiency.

**Baselines.** We compare MAG to state-of-the-art models trained for both generic and molecule generation. Specifically, baselines include diffusion models, such as EDP-GNN [6], GDSS [7], and DiGress [8]; hybrid models, such as GraphAF [15], GraphDF [24] and GraphRNN [3] (generic graphs only); and VAE models, such as GraphVAE [25] and GramVAE [26] (molecular graphs only).

### 4.1 Generic Graph Generation

**Experimental Setup.** We evaluate MAG at generic graph generation on the Community-small [7] and Enzymes [27] datasets. The former is a synthetic dataset containing 100 random graphs consisting of two equal-sized communities, with between 12 and 20 nodes per graph; while the latter contains 587 protein graphs with 10 to 125 nodes per protein.

These datasets provide a wide range of graph properties, from small structured communities in Community-small to larger and more complex protein graphs in Enzymes. We aim to investigate the ability of multi-scale graph generation to generate graphs of different sizes and complexities, providing insights into its scalability and generalization abilities.

To ensure fair comparison, we follow the same setup as [7, 9, 11], randomly splitting the dataset into 80% for training and 20% for testing. Performance is evaluated by comparing the structure of the generated graphs with those from the dataset according to the maximum mean discrepancy (MMD) of statistics including node degrees, clustering coefficients, and orbit counts. Furthermore, the inference speed of MAG is compared to the baselines at generating graphs of varying sizes. Samples of generated graphs are displayed in Figure 4.

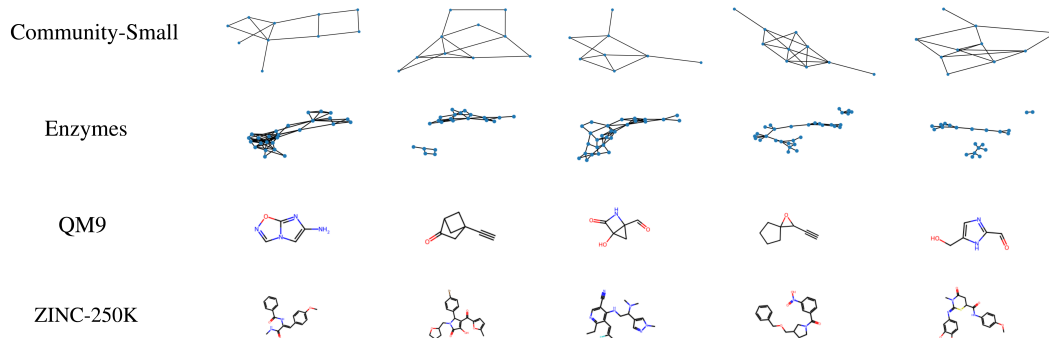


**Figure 4:** Samples of generated generic and molecular graphs by MAG.

**Table 1:** Quantitative results on **Community-small** and **Enzymes** benchmark datasets. Inference times are reported in seconds for 50 and 100 samples, respectively, on an NVIDIA GeForce RTX 4060 GPU. Orbit results are missing due to computational incompatibility.

Models	Community-S ( $ \mathcal{V}  \in [12, 20]$ , 100 obs.)				Enzymes ( $ \mathcal{V}  \in [10, 125]$ , 587 obs.)			
	Deg. $\downarrow$	Clus. $\downarrow$	Orbit. $\downarrow$	Time $\downarrow$	Deg. $\downarrow$	Clus. $\downarrow$	Orbit. $\downarrow$	Time $\downarrow$
<i>Diffusion Models</i>								
EDP-GNN	0.053	0.144	0.026	$1.94e^4$	0.023	0.268	0.082	$2.61e^4$
GDSS	<b>0.045</b>	0.086	0.007	$2.87e^3$	0.026	0.061	0.009	$1.74e^3$
DiGress	0.047	<b>0.041</b>	0.026	38.1	0.004	0.083	0.002	58.8
<i>Hybrid Models</i>								
GraphAF	0.180	0.200	0.020	$1.29e^2$	1.669	1.283	0.266	46.1
GraphDF	0.060	0.120	0.030	68.8	1.503	1.061	0.202	68.1
GraphRNN	0.080	0.120	0.040	$1.10e^2$	0.017	0.062	0.046	$1.25e^2$
<i>Varational Autoencoders</i>								
GraphVAE	0.350	0.980	0.540	1.34	1.369	0.629	0.191	2.00
<b>Ours</b>	0.077	0.102	–	<b>0.187</b>	1.753	1.148	–	<b>1.88</b>

**Results.** Table 1 presents the quantitative MMD results comparing our proposed method to baseline models. MAG demonstrates the ability to generate high-quality samples that closely resemble the original data. On the smaller Community-small dataset, MAG consistently outperforms hybrid models and VAEs. Notably, its performance approaches that of state-of-the-art GDSS and DiGress models.

For the more complex Enzymes dataset, MAG further surpasses hybrid and VAE baselines in both performance and computational efficiency. Hybrid approaches struggle with larger enzymes, highlighting scalability limitations, whereas MAG enjoys strong scalability from its autoregressive nature. Consequently, our method achieves performance comparable to diffusion-based approaches on these.

In terms of computational efficiency, inference time evaluation reveals significant improvements across all datasets, surpassing all baselines by several orders of magnitude. Remarkably, compared to state-of-the-art models, MAG achieves inference speeds of up to **thousands of times faster**.

## 4.2 Molecule Generation

**Experimental Setup.** MAG is further extended to generate molecular graphs with node and edge features, and evaluated on two popular molecular datasets, namely QM9 [28] and ZINC-250K [29]. The former contains 133,885 small organic molecules of up to nine heavy atoms with types C, O, N and F. The latter is a subset of the ZINC database and consists of 250,000 molecules with up to 38 heavy atoms of nine types.

In contrast to generic graph generation, molecules present a unique challenge for multi-scale graph generation due to their strict structural constraints and varying complexity. Evaluating MAG on both molecular datasets assesses its ability to generate realistic molecules ranging from small organic compounds to larger chemical structures, while adhering to chemical constraints like valency, introducing additional challenges for the model to maintain validity.

The quality of generated molecules is measured in terms of validity, uniqueness, novelty, and Fréchet ChemNet Distance (FCD). Details on these metrics are delineated in Appendix B. In addition, the inference time to generate 1,000 molecules from both datasets is recorded and compared against baselines. Samples of generated molecules are displayed in Figure 4.

**Table 3:** Quantitative results on **QM9** and **ZINC250k** molecule datasets.

Models	QM9 ( $ \mathcal{V}  \in [1, 9]$ , 134K mols.)				ZINC250k ( $ \mathcal{V}  \in [6, 38]$ , 250K mols.)			
	Valid $\uparrow$	Unique $\uparrow$	Novel $\uparrow$	FCD $\downarrow$	Valid $\uparrow$	Unique $\uparrow$	Novel $\uparrow$	FCD $\downarrow$
<i>Diffusion Models</i>								
EDP-GNN	47.52	99.25	86.58	2.68	82.97	<b>99.79</b>	100	16.74
GDSS	95.72	98.46	86.27	2.9	<b>97.01</b>	99.64	100	<b>14.66</b>
DiGress	<b>99.0</b>	96.66	33.4	<b>0.36</b>	91.02	81.23	100	23.06
<i>Hybrid Models</i>								
GraphAF	74.43	88.64	86.59	5.27	68.47	98.64	100	16.02
GraphDF	93.88	98.58	98.54	10.93	90.61	99.63	100	33.55
<i>Varational Autoencoders</i>								
GramVAE	20.00	19.70	<b>100</b>	–	30.10	27.30	100	–
GraphVAE	45.80	30.50	66.10	–	44.00	–	–	–
<b>Ours</b>	80.28	<b>99.68</b>	83.14	3.42	77.27	86.27	100	16.88

**Results.** Qualitative results on molecular datasets are given in Table 3. These results showcase MAG’s ability to generate high-quality molecules that respect imposed chemical constraints. As observed, the proposed method surpasses VAE baselines across most metrics. Furthermore, MAG enjoys performance competitive to those of hybrid models.

As for the larger, more complex ZINC-250k dataset, MAG surpasses VAE baselines across all metrics and offers comparable results to hybrid models, falling just short of those posed by diffusion models. These results demonstrate that, although MAG is able to effectively generate realistic molecules while adhering to chemical structural constraints, its performance is slightly reduced on complex molecules.

With regards to computational efficiency, drastic improvements in inference time evaluation remain consistent for molecular graphs, surpassing all baselines by at least one order of magnitude and achieving inference speeds of up to **hundreds of times faster**.

## 5 Future Work

This work primarily focused on introducing a novel paradigm for autoregressive graph generation, adopting a *next-scale* prediction approach instead of traditional *next-node* and *next-edge* methods. As a result, a promising avenue for future research is to explore how autoregressive properties from the large language model (LLM) literature translate to graph generation. Specifically, efforts could be made to investigate the generalization capabilities of autoregressive models in zero-shot and few-shot downstream tasks, as well as their scalability to larger graphs.

Additionally, incorporating inductive biases into the graphs’ scales based on domain-specific knowledge or additional contextual information could further enhance model performance and applicability.

Finally, this work opens a new direction for hybrid autoregressive-diffusion methods. While current hybrid approaches primarily rely on block-wise diffusion with sequential learning between blocks, the proposed framework enables reconsidering these methods by applying scale-wise diffusion, i.e.,

**Table 2:** Comparison of generation times using NVIDIA GeForce RTX 4060 on molecular datasets. Times are reported in seconds for 1,000 samples.

Models	Molecular graphs	
	QM9	ZINC250K
EDP-GNN	$1.74e^3$	$1.62e^3$
GDSS	43.4	$3.44e^2$
DiGress	34.1	$2.03e^2$
GraphAF	$1.05e^3$	$9.61e^2$
GraphDF	$1.93e^4$	$9.29e^3$
<b>Ours</b>	<b>3.84</b>	<b>19.7</b>

diffusion between scales. This shift could eliminate the need for quantization, as diffusion offers strong capabilities in continuous space, thereby removing the autoencoder’s quantization bottleneck. However, this would reintroduce computational overheads which should be studied against existing diffusion-based approaches.

## 6 Conclusion

We introduced a novel diffusion-free multi-scale autoregressive model for graph generation which (1) theoretically addresses limitations of traditional autoregressive (AR) models due to inherent graph properties, and (2) reduces the gap between diffusion-free transformer-based AR models and diffusion-based methods, with up to three orders of magnitude lower computational costs. Experiments over both generic and molecular graph generations demonstrate the ability of MAG to generate high-quality samples that achieve competitive performance with state-of-the-art models and adjust to domain-specific constraints such as chemical validity. We hope that our findings can aid the design of new approaches, in which the multi-scale paradigm may be applied to other graph generative methods.

## Acknowledgements

We would like to thank Miruna Cretu, Charlie Harris, and Karolis Martinkus for their guidance and valuable feedback throughout this work.

## References

- [1] Keyu Tian, Yi Jiang, Zehuan Yuan, Bingyue Peng, and Liwei Wang. Visual autoregressive modeling: Scalable image generation via next-scale prediction. In *Proceedings of the 38th Annual Conference on Neural Information Processing Systems*, 2024. [1](#), [2](#), [4](#)
- [2] Sucheng Ren, Qihang Yu, Ju He, Xiaohui Shen, Alan Yuille, and Liang-Chieh Chen. Beyond next-token: Next-x prediction for autoregressive visual generation. *arXiv preprint arXiv:2502.20388*, 2025. [1](#), [2](#)
- [3] Jiaxuan You, Rex Ying, Xiang Ren, William Hamilton, and Jure Leskovec. Graphrnn: Generating realistic graphs with deep autoregressive models. In *Proceedings of the 35th International Conference on Machine Learning*, pages 5708–5717. PMLR, 2018. [1](#), [2](#), [3](#), [6](#)
- [4] Wengong Jin, Regina Barzilay, and Tommi Jaakkola. Junction tree variational autoencoder for molecular graph generation. In *Proceedings of the 35th International Conference on Machine Learning*, volume 80, pages 2323–2332. PMLR, July 2018. [1](#), [3](#)
- [5] Nicola De Cao and Thomas Kipf. Molgan: An implicit generative model for small molecular graphs. *arXiv preprint arXiv:1805.11973*, 2018. [1](#)
- [6] Chenhao Niu, Yang Song, Jiaming Song, Shengjia Zhao, Aditya Grover, and Stefano Ermon. Permutation invariant graph generation via score-based generative modeling. In *Proceedings of the 23rd International Conference on Artificial Intelligence and Statistics (AISTATS)*, 2020. [1](#), [3](#), [6](#)
- [7] Jaehyeong Jo, Seul Lee, and Sung Ju Hwang. Score-based generative modeling of graphs via the system of stochastic differential equations. *arXiv preprint arXiv:2202.02514*, 2022. [1](#), [3](#), [6](#)
- [8] Clement Vignac, Igor Krawczuk, Antoine Siraudin, Bohan Wang, Volkan Cevher, and Pascal Frossard. Digress: Discrete denoising diffusion for graph generation. In *Proceedings of the Eleventh International Conference on Learning Representations*, 2023. [1](#), [3](#), [5](#), [6](#)
- [9] Lingkai Kong, Jiaming Cui, Haotian Sun, Yuchen Zhuang, B. Aditya Prakash, and Chao Zhang. Autoregressive diffusion model for graph generation. In *Proceedings of the 40th International Conference on Machine Learning (ICML)*, pages 17391–17408. PMLR, 2023. [1](#), [3](#), [6](#)
- [10] Lingxiao Zhao, Xueying Ding, and Leman Akoglu. Pard: Permutation-invariant autoregressive diffusion for graph generation. In *Proceedings of the 38th Annual Conference on Neural Information Processing Systems*, 2024. [1](#), [3](#)

[11] Qi Yan, Zhengyang Liang, Yang Song, Renjie Liao, and Lele Wang. Swingnn: Rethinking permutation invariance in diffusion models for graph generation. *Transactions on Machine Learning Research*, 2024. 1, 3, 6

[12] Tom Henighan, Jared Kaplan, Mor Katz, Mark Chen, Christopher Hesse, Jacob Jackson, Heewoo Jun, Tom B Brown, Prafulla Dhariwal, Scott Gray, et al. Scaling laws for autoregressive generative modeling. *arXiv preprint arXiv:2010.14701*, 2020. 1

[13] Victor Sanh, Albert Webson, Colin Raffel, Stephen H Bach, Lintang Sutawika, Zaid Alyafeai, Antoine Chaffin, Arnaud Stiegler, Teven Le Scao, Arun Raja, et al. Multitask prompted training enables zero-shot task generalization. *arXiv preprint arXiv:2110.08207*, 2021. 2

[14] Renjie Liao, Yujia Li, Yang Song, Shenlong Wang, William Hamilton, David K. Duvenaud, Raquel Urtasun, and Richard Zemel. Efficient graph generation with graph recurrent attention networks. In *Advances in Neural Information Processing Systems*, volume 32, 2020. 2, 3

[15] Chence Shi, Minkai Xu, Zhaocheng Zhu, Weinan Zhang, Ming Zhang, and Jian Tang. Graphaf: A flow-based autoregressive model for molecular graph generation, 2020. 2, 6

[16] Yujia Li, Oriol Vinyals, Chris Dyer, Razvan Pascanu, and Peter Battaglia. Learning deep generative models of graphs. *arXiv preprint arXiv:1803.03324*, 2018. 3

[17] Xiaohui Chen, Xu Han, Jiajing Hu, Francisco Ruiz, and Liping Liu. Order matters: Probabilistic modeling of node sequence for graph generation. In *Proceedings of the 38th International Conference on Machine Learning*, pages 1630–1639. PMLR, 2021. 3

[18] Xiaoyang Hou, Tian Zhu, Milong Ren, Dongbo Bu, Xin Gao, Chunming Zhang, and Shiwei Sun. Improving molecular graph generation with flow matching and optimal transport, 2024. 3

[19] Andreas Bergmeister, Karolis Martinkus, Nathanaël Perraudin, and Roger Wattenhofer. Efficient and scalable graph generation through iterative local expansion. In *Proceedings of the 12th International Conference on Learning Representations*, 2024. 3

[20] Wengong Jin, Regina Barzilay, and Tommi Jaakkola. Hierarchical generation of molecular graphs using structural motifs. In *Proceedings of the International Conference on Machine Learning*, 2020. 3

[21] Alex O Davies, Nirav S Ajmeri, et al. Size matters: Large graph generation with higgs. *arXiv preprint arXiv:2306.11412*, 2023. 3

[22] Jacob Devlin, Ming-Wei Chang, Kenton Lee, and Kristina Toutanova. BERT: Pre-training of deep bidirectional transformers for language understanding. In *Proceedings of the 2019 Conference of the North American Chapter of the Association for Computational Linguistics: Human Language Technologies, Volume 1 (Long and Short Papers)*, June 2019. 5

[23] Chengxuan Ying, Tianle Cai, Shengjie Luo, Shuxin Zheng, Guolin Ke, Di He, Yanming Shen, and Tie-Yan Liu. Do transformers really perform badly for graph representation? In *Advances in Neural Information Processing Systems*, 2021. 5

[24] Youzhi Luo, Keqiang Yan, and Shuiwang Ji. Graphdf: A discrete flow model for molecular graph generation, 2021. 6

[25] Martin Simonovsky and Nikos Komodakis. Graphvae: Towards generation of small graphs using variational autoencoders. In *Artificial Neural Networks and Machine Learning–ICANN 2018: 27th International Conference on Artificial Neural Networks, Rhodes, Greece, October 4–7, 2018, Proceedings, Part I* 27, pages 412–422. Springer, 2018. 6

[26] Matt J Kusner, Brooks Paige, and José Miguel Hernández-Lobato. Grammar variational autoencoder. In *International conference on machine learning*, pages 1945–1954. PMLR, 2017. 6

[27] Ida Schomburg, Antje Chang, Oliver Hofmann, Christian Ebeling, Frank Ehrentreich, and Dietmar Schomburg. Brenda, the enzyme database: Updates and major new developments. *Nucleic Acids Research*, 32(Database issue):D431–D433, 2004. doi: 10.1038/nar/gkh081. 6

[28] Raghunathan Ramakrishnan, Pavlo O. Dral, Matthias Rupp, and O. Anatole von Lilienfeld. Quantum chemistry structures and properties of 134 kilo molecules. *Scientific Data*, 1:140022, August 2014. doi: 10.1038/sdata.2014.22. 7

[29] John J. Irwin, Teague Sterling, Michael M. Mysinger, Erin S. Bolstad, and Ryan G. Coleman. Zinc: A free tool to discover chemistry for biology. *Journal of Chemical Information and Modeling*, 52(7):1757–1768, July 2012. doi: 10.1021/ci3001277. 7

## A Proof of Complexity Reduction

This proof entails the improvement in generation complexity from node-by-node to scale-wise AR models.

**Lemma 1** (AR Generation for Nodes). *For a standard self-attention transformer, the time complexity of autoregressive (AR) graph generation is  $O(N^3)$ , where  $N$  is the total number of nodes.*

*Proof.* In AR generation, nodes are generated sequentially. At step  $i$  ( $1 \leq i \leq N$ ), the model computes attention over all  $i - 1$  previously generated nodes. The complexity for step  $i$  is  $O(i^2)$ . Summing over all steps:

$$\sum_{i=1}^N i^2 = \frac{N(N+1)(2N+1)}{6} \sim O(N^3).$$

□

**Lemma 2** (Scale-wise Generation for Nodes). *For a standard self-attention transformer with constant  $a > 1$ , the time complexity of variable autoregressive (VAR) graph generation is  $O(N^2)$ , where  $N$  is the total number of nodes, and  $K = \log_a N + 1$  scales are used.*

*Proof.* Define the resolution sequence  $\{n_k\}$ , where  $n_k = a^{k-1}$  nodes are added at scale  $k$ , and  $n_K = N$ . The total nodes up to scale  $k$  is:

$$S_k = \sum_{i=1}^k n_i = \frac{a^k - 1}{a - 1}.$$

At each scale  $k$ , generating  $n_k$  new nodes requires computing attention over all  $S_{k-1}$  existing nodes. The complexity is:

$$n_k \cdot S_{k-1} \approx a^{k-1} \cdot a^{k-1} = a^{2(k-1)}.$$

Summing over all  $K$  scales:

$$\sum_{k=1}^K a^{2(k-1)} = \frac{a^{2K} - 1}{a^2 - 1} \sim O(a^{2K}) = O(N^2),$$

since  $a^{K-1} = N$  and thus  $a^{2K} = a^2 N^2$ .

□

## B Details for Evaluation Metrics

To evaluate the performance of MAG for generic graphs, we measure the degree, clustering, and orbit of the generated graphs. Degree measures the number of connections of each node, revealing hubs or sparsely connected regions. Clustering shows how likely a node's neighbors are to be connected, indicating local group structures or tightly-knit communities. Orbit counts specific small patterns (subgraphs) within the graph, capturing repeating structural patterns. These metrics report whether the structure of the graphs in the dataset is preserved, indicating more meaningful and realistic graphs.

We evaluate the performance on molecular graphs by measuring uniqueness, novelty, validity, FCD, and NSPDK. Uniqueness and novelty ensure that the model can extrapolate to new molecules rather than overfitting the training data, while validity verifies whether generated molecules follow fundamental chemical rules, such as valency constraints. In addition, FCD measures how closely the generated molecules resemble real compounds in terms of learned chemical properties, while NSPDK evaluates structural similarity at the subgraph level.